metals

MDPI

Article

The Effect of Misalignment on Stress Concentration and Fatigue Life for Circumferential Weld Joints of Pipeline

Niantao Zhang [1,2,3], Caiyan Deng [1,2], Zhichen Lin [1,2], Zhijiang Wang [1,2,*] and Shaojie Wu [1,2]

1 School of Materials Science and Engineering, Tianjin University, Tianjin 300350, China; 1016208055@tju.edu.cn (N.Z.); dengcy@tju.edu.cn (C.D.); linzhichen4396_@tju.edu.cn (Z.L.); shaojie@tju.edu.cn (S.W.)
2 Tianjin Key Laboratory of Advanced Joining Technology, Tianjin 300350, China
3 Offshore Oil Engineering Co., Ltd., Tianjin 300456, China
* Correspondence: wangzj@tju.edu.cn

Abstract: Misalignment has a significant impact on the fatigue performance of circumferential weld joints in pipelines, which can significantly reduce the fatigue life. Misalignment generates a structural stress concentration on the pipeline, which proportionally reduces its fatigue strength. Moreover, due to the misalignment, the reinforcement of the root and the transition angle of the pipeline inwall are significantly reduced, increasing its notch stress concentration factor and further reducing its fatigue performance. This work investigates the effect of misalignment on stress concentration in the circumferential welds of pipelines, and it is used to predict the fatigue life. The structural stress method is proposed in the present work, and finite element analysis technology with Abaqus is used to calculate the structural stress concentration factor k_j at the root-pass toe of misaligned circumferential weld joints, and a formula for the relationship between the structural stress concentration factor k_j and the misalignment is established. The total stress concentration factor k of weld joints with different misalignments under several welding processes are calculated, and are compared with the structural stress concentration factor k_j. The fatigue test data of weld joints with different misalignments are studied, and it is shown that the fatigue performance could be predicted by the fitting result.

Keywords: misalignment; finite element method; structural stress method; stress concentration factor; fatigue performance

check for updates

Citation: Zhang, N.; Deng, C.; Lin, Z.; Wang, Z.; Wu, S. The Effect of Misalignment on Stress Concentration and Fatigue Life for Circumferential Weld Joints of Pipeline. *Metals* **2024**, *14*, 545. https://doi.org/10.3390/met14050545

Academic Editor: Antonio Mateo

Received: 29 March 2024
Revised: 26 April 2024
Accepted: 1 May 2024
Published: 4 May 2024

1. Introduction

Welded structures are an important component of long-distance transportation pipelines, and welding is the most important joining method for pipelines. However, misalignment (including axial misalignment and angular misalignment) during the fitting-up process often leads to residual stress and the formation of stress concentration areas, resulting in a significant decrease in the fracture toughness and fatigue performance of the welded structure, and creating potential accident-prone areas [1,2].

The experimental measurement of residual stress in circumferential weld joints is cumbersome. Ma et al. [3] addressed the issue of high residual stress in pipelines and low measurement accuracy using the blind hole method. They fitted the variation of strain release coefficient with the ratio of the applied stress to the yield strength of the specimen, improving the accuracy of the blind hole method in measuring high residual stress and providing a reference value for engineering applications of the blind hole method. Halabuk et al. [4] used the drilling method to measure residual stresses in cylindrical components and proposed a new finite element method (FEM) for applying loads to drilling tests. By simulating several cylinders with different residual stress states and evaluating the results according to the ASTM E837 standard [5], the influencing factors were determined, and the residual stress errors of several cylinders were quantified. Hong et al. [6] used a new load measurement method to measure residual stress loads, and analyzed the residual stress of injection-molded car lamp parts. They compared the results with the drilling method, and found that the residual stress on the surface of the lampshade tested by the two methods was very close. Tajdary et al. [7] considered the inherent mean effect in residual stress X-ray diffraction (XRD) measurements, which is related to the finite size of the irradiation area, resulting in inaccurate measurements in the presence of high surface stress gradients. A deconvolution stress reconstruction method based on average XRD measurements was proposed, which allowed for the drawing of non-uniform residual stress maps based on XRD measurements. Li et al. [8] used electron diffraction to measure residual stress in welds. In their study, electronic speckle interference (ESPI) was used to measure residual stress in A36 specimens from the American Society for Testing and Materials by carbon dioxide welding. The residual stress of the welding part was obtained from the phase diagram image obtained from ESPI. The results confirmed that the residual stress of welded components can be measured by ESPI. Nitschke-Pagel [9] considered that residual stress measurement techniques using different diffraction methods have certain limitations, especially relating to factors such as materials, welding types, and sizes, that affect the quality of measurement results and the measurement environment. Therefore, XRD cyclic testing of weld joints was used for analysis.

With the development of FEMs and computer technology, obtaining residual stress values with FEMs has become popular, as it represents a methodology in which the specimen or component will not be destroyed. Eftekhar [10] analyzed the effects of various heat source models on welding temperature and residual stress using the SYSWELD software, and found that the three-dimensional (3D) Gaussian and double elliptical heat source models predicted thermal cycling and residual stress more accurately. Maarten et al. [11] used numerical simulation and experimental measurement to study the numerical values and distribution of residual stress, and explored the effects of latent heat in phase transformation and volume strain on welding residual stress. Venkata et al. [12] analyzed the P91-steel butt joint and established a numerical model to simulate the residual stress in the butt joint under different heat treatment parameters, and conducted experimental verification. The developed model and the predictions were validated using neutron diffraction measurements on as-welded and post-weld heat-treated plates. A good agreement was achieved between the measurements and predictions. Xu et al. [13] used numerical simulation methods to calculate the residual stress and welding deformation of aluminum-alloy welds. Through experiments, the actual temperature field and deformation of the welded structure were measured, and the differences between the two were compared and analyzed to verify the accuracy of the simulation results. Cheng et al. [14] studied L415 pipeline steel and conducted numerical simulations on the temperature and stress fields during gas pipeline welding using the Ansys software. The research results indicated that applying a strip heat source, in the form of heat generation rate, can effectively calculate the residual stress field of welding. Zhao et al. [15] established a 3D full-scale finite element model of an X80 steel pipe and predicted the welding stress distribution of four typical ring joints. The calculated results were compared with the actual drilling data and showed a high reliability.

Usually, when calculating the stress concentration factor, it is necessary to cut the pipeline to measure the shaping parameters, such as the angular deformation. Thus, it would be beneficial to calculate the stress concentration factor without breaking the pipeline, with the help of FEMs.

There are currently two commonly used research methods for fatigue life analysis of weld joints. One is the nominal stress method, which uses S–N curves that plot applied stress (S) against component life or number of cycles to failure (N) for different standards and different structures to assess fatigue life [16–19]. Another method is the fracture mechanics method, which is based on the crack propagation rate [20]. Jiang et al. [21] analyzed the mechanism of residual stress redistribution under cyclic loading and its impact on fatigue performance based on experimental measurements of residual stress. The results showed that the effect of residual stress on fatigue life was mainly reflected by the increase in average stress, and the increase in magnitude depended on the redistribution of stress. A fatigue prediction model for weld joints was proposed, and the predicted lives were within the 1.5% error band. Pokorny et al. [22] proposed a fatigue life assessment method for axles under external loads and residual stress, and analyzed the effect of heat treatment on the structure. Residual fatigue life was calculated for various starting crack lengths based on the experimentally determined Paris curves for various load ratios. The data calculated using the fatigue life assessment method for the axle was smaller than the experimental data, which ensured that the axle would not fracture earlier than expected. Barsoum et al. [23] developed a welding simulation program using the Ansys software to predict residual stress and combined it with the Forman formula, considering the influence of residual stress to predict the fatigue life of multi-pass butt welded plates and T-shaped fillet welds. Cui et al. [24] proposed a fatigue life prediction model based on linear elastic fracture mechanics, which considers welding residual stress and calculates the residual stress intensity factor using the weight function method.

In order to predict the fatigue performance of weld joints without damaging the weld, this work combines the structural stress method with the equivalent notch stress concentration factor and uses it to calculate the stress concentration factor of pipeline circumferential welding. The combination of finite element simulation and the structural stress method considers the stress mutation caused by the structural stress concentration [25], which can effectively predict and analyze the residual stress and stress concentration factor, and reduce the width of the S–N curve [26]. Finally, this calculation result is used for predicting the fatigue life.

2. Materials and Method

2.1. Materials and Welding Procedures

The base material was X65 pipeline steel, with dimensions of diameter (Φ) 355 mm $\times$ thickness 19.1 mm. The filling material was ER80S-G solid wire (ESAB Corporation, North Bethesda, MD, United States), with a dimension of Φ1.0 mm. The main chemical composition of the base material and filling material is shown in Table 1. The mechanical properties of the base material are shown in Table 2. Circumferential butt joints, with a V-shaped groove, were prepared. During welding, gas metal arc welding (GMAW) was used for root, filling, and cap passes. The groove parameters are shown in Figure 1, with a groove angle of 50°, and a root face height of 1.0 mm.

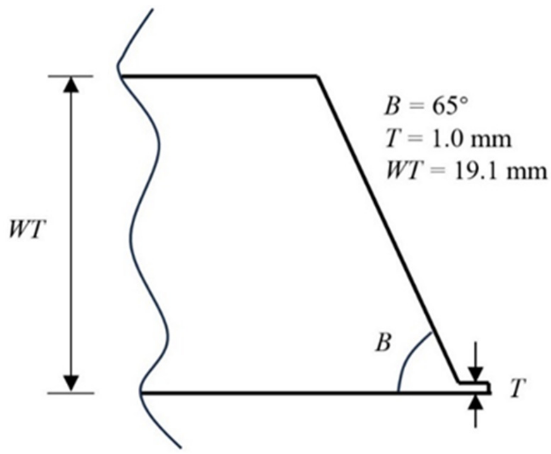

Figure 1. Groove parameters for the butt pipe joint.

Table 1. Chemical composition for base and filling materials.

Material	C	Mn	Si	S	P	Fe
X65	0.050	1.400	0.220	0.050	0.040	Balance
ER80S-G	0.080	1.640	0.540	0.006	0.012	Balance

Table 2. Mechanical properties of the base material.

Material	Yield Strength Min (MPa)	Yield Strength Max (MPa)	Tensile Strength Min (MPa)	Poisson's Ratio	Young's Modulus (GPa)	Elongation (%)
X65	480.0	560.0	531.0	0.3	210	30.7

2.2. Finite Element Method for Stress Concentration Factor

The numerical simulation software Abaqus is widely used in the field of welding. It can be used to simulate the temperature field and stress field during the welding process, including in fatigue tests of weld joints, etc. [27]. The Abaqus (2022) software and the structural stress method are combined in the present work to calculate the stress concentration factor of structures with misalignments.

During the modeling process, based on the experimental welding results, the misalignment and the reinforcement of the root pass were measured for finite element modeling. The geometry of the fatigue specimens was as shown in Figure 2. The mechanical properties that were used in the modeling are listed in Table 2. The mechanical properties for the weld joints and base materials were the same in the modeling. The test stress level of the specimen was determined by the stress level of the full-size specimen specified in DEP 37.81.40.31-Gen [28] and the maximum tensile residual stress obtained from the weld metal zone and the heat affected zone.

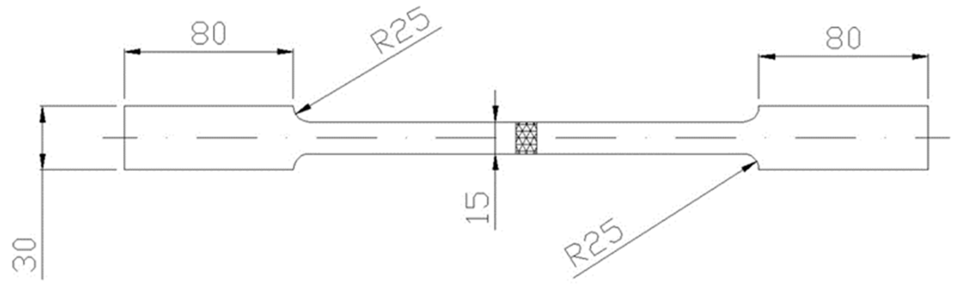

Figure 2. Fatigue specimen size (Unit: mm).

To compensate for the released residual stress, a portable X-ray diffractometer (Xstress3000 by Stresstech Group, Vaajakoski, Finland) was used to test the residual stress on the surface of the weld metal and heat affected zone of the X65 pipeline. The measurement results showed that the maximum residual stress occurred at 6 o'clock, 10 mm away from the weld center, with a residual stress of 260.0 MPa. For conservative considerations, a maximum residual tensile stress of 260.0 MPa was selected for the load compensation. The fixed static load was 400.0 MPa, and the dynamic loads were at three stress levels of 175.0 MPa, 120.0 MPa, and 80.0 MPa. The stress level data of the fatigue test for the X65 pipeline are shown in Table 3. The maximum stress added was 487.5 MPa, while the minimum yield strength of the X65 steel was 480.0 MPa, and the tensile strength was 531.0 MPa. The material did not undergo plastic deformation due to tensile stress, and the amount of elastic deformation that occurred was also relatively small. Therefore, it was assumed that tensile stress did not affect stress concentration by deforming the specimens.

Table 3. Test stress level in fatigue tests.

Mean Stress (MPa)	Stress Range (MPa)	Maximum Stress (MPa)	Minimum Stress (MPa)	Maximum Stress after Residual Stress Correction (MPa)	Minimum Stress after Residual Stress Correction (MPa)
140.0	175.0	227.5	52.5	487.5	312.5
140.0	120.0	200.0	80.0	460.0	340.0
140.0	80.0	180.0	100.0	440.0	360.0

In the field output request of the Create Step dialog box, NFORC, i.e., the node force caused by element stress, was selected as the field output for the subsequent structural stress calculation. In the Load Create step, the load was applied by fixing one end of the specimen and adding periodic dynamic loads to the other end. The meshing of the model followed the rule that the grids (C3D8) were sparse at both ends, and were dense in the middle. In the direction of the x-axis, the grid widths for the weld joint, the area near the weld joint, the transition area, and the area away from the weld joint were 1 mm, 2 mm, 4 mm, and 16 mm, respectively. The grid width in the direction of the y-axis was 1.2 mm. At the same time, considering that the stress calculation was calculated in 2D mode, the grid division was not conducted in the direction of z-axis. The meshing result is shown in Figure 3.

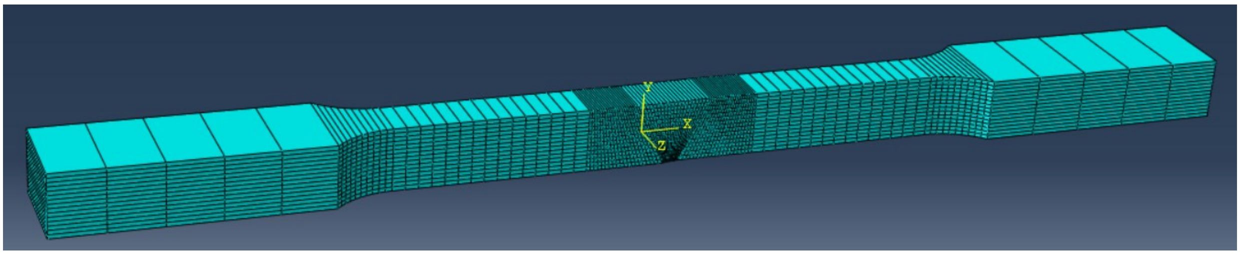

Figure 3. Meshing for the FEM.

In the visualization step, according to the requirements of structural stress calculation, three continuous unit blocks were taken at the toe and at the far end as isolation bodies, and one end of the isolation body path was taken to obtain the corresponding relationship between nodes and node forces on the path. A typical stress map from post-processing is shown in Figure 4.

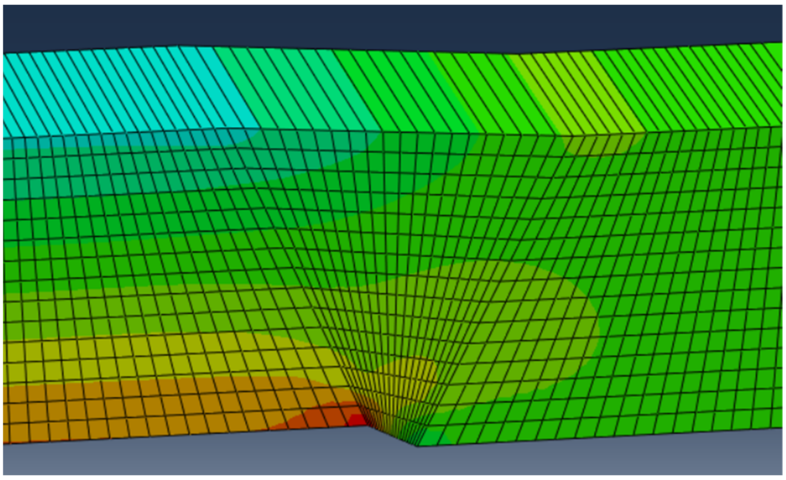

Figure 4. Typical stress map.

The existence of weld joints can cause geometric discontinuity in a structure, leading to local stress concentration and even a stress singularity; that is, the theoretical stress at the toe tends to be infinity. This can cause the stress at the toe to increase as the grid size decreases in finite element calculations, resulting in nonconvergence of the grid at the toe. Nominal stress cannot describe the common fatigue issues for different types of joints, as it is away from the fatigue crack surface. In this regard, a structural stress method based on the node force calculation by a finite element model was used to correct the structural stress parameters, obtaining the equivalent structural stress. The specific formula [29] is as follows.

Plane modulus stress at the toe is:

$$\sigma_m = \frac{1}{t} \times \int_{-t/2}^{t/2} \sigma_x(y)\mathrm{d}y \tag{1}$$

where t is the thickness of the sample, and σ_x is the nodal force.

Plane bending stress at the toe is:

$$\sigma_b = \frac{6}{t^2} \times \int_{-t/2}^{t/2} \sigma_x(y)y\mathrm{d}y \tag{2}$$

Equivalent structural stress is:

$$S_s = \frac{|\ \sigma_s\ |}{t^{(2-m)/(2m)} \times I(r)^{1/m}} \tag{3}$$

where $|\ \sigma_s\ | = |\ \sigma_m\ | + |\ \sigma_b\ |$, which is the sum of the modulus stress and bending stress; $I(r)^{1/m}$ is the correction of the bending stress ratio; $t^{(2-m)/(2m)}$ is the thickness correction; and $m = 3.6$.

2.3. Experimental Mothods for Stress Concentration Factor

In order to verify the accuracy of the structural stress concentration factor, small specimens with dimensions as shown in Figure 2 were sampled from the pipeline, and the shaping parameters, such as the welding angular deformation of the specimen, were measured.

Respectively, the stress concentration factor caused by axial misalignment $k_{m,axial}$ and the stress concentration factor caused by angular misalignment $k_{m,angular}$ were calculated. Then, the stress concentration factor caused by total misalignment k_m was calculated. The calculation method [30] is shown in Equations (4)–(6).

$$k_{m,axial} = 1 + 6\frac{el_1}{t(l_1 + l_2)} \tag{4}$$

where e is the misalignment; and l_1 and l_2 are the widths on both sides of the weld joint.

$$k_{m,angular} = 1 + \frac{3\alpha l}{t} \times \frac{\tan\mathrm{h}(\beta)}{\beta} \tag{5}$$

where $\beta = \frac{2l}{t}\sqrt{\frac{3\sigma_m}{E}}$ (in which σ_m is the radial stress and E is the elastic modulus); α is an angle expressed in radians; and l is half of the length of the specimen.

$$k_m = 1 + \left(k_{m,axial} - 1\right) + \left(1 - k_{m,angular}\right) \tag{6}$$

The parameters, such as transition radius and transition angle at the toe of the root pass, were measured. Then, the equivalent notch stress concentration factor k_t, caused by the shape of the weld joint and based on the empirical Equation (7), proposed by Pachoud et al. [31], was calculated.

$$k_t^{\rho} = 1 + \alpha_0\left(\frac{\delta}{t_s}\right)^{\alpha_1}\left(\frac{r_{ref}}{t_s}\right)^{\alpha_2}\tan\left(\frac{\beta}{2}\right)^{\alpha_3} \tag{7}$$

where $\alpha_0 = 0.99$; $\alpha_1 = 0.06$; $\alpha_2 = -0.34$; $\alpha_3 = 0.59$; the toe transition radius $\rho = r_{ref} = 1$ mm; t_s is the thickness of the pipeline; β is the side angle of the toe; and δ is the reinforcement at the backside of the weld joint. The total stress concentration factor k is represented by Equation (8).

$$k = k_m \cdot k_t \tag{8}$$

3. Results and Discussion

3.1. Stress Concentration Factor Calculation Results by Finite Element Method

The equivalent structural stress and structural stress concentration factor k_j, which were calculated by Equations (1)–(3), are shown in Table 4. Among them, the stress concentration factor is the ratio of the equivalent structural stress at the toe over that at the far end.

Table 4. Stress concentration factor under the dynamic load of 175 MPa.

Misalignment (mm)	S_s at the Toe (MPa)	S_s (MPa)	Structural Stress Concentration Factor k_j
0.5	1890.4	1076.7	1.756
0.8	2127.8	1082.9	1.965
1.0	2318.5	1082.9	2.141
1.2	2490.7	1082.9	2.300
1.5	2689.7	1082.9	2.484

By using the least squares method, the misalignment and stress concentration factor k_j were fitted as a quadratic function, and the coefficients of the quadratic function are shown in Table 5. The residual sum of squares (*RSS*) was 2.384×10^{-17}, indicating a good fitting effect and an acceptable accuracy range.

Table 5. Fitting result between the misalignment and stress concentration factor.

Quadratic Term	Linear Term	Constant Term	*RSS*
0.042	0.688	1.403	2.384×10^{-17}

It can be seen from the finite element calculation results that when the misalignment was small, the stress concentration coefficient k_j changed more slowly as the misalignment increased. This was because the X65 pipeline steel had a strong resistance to deformation, which was reflected in the setting of the elastic modulus. Strong resistance to deformation means that when subjected to axial stretching, the material has a relatively small axial elongation and vertical shrinkage. This results in a small difference in the ratio of misalignment to pipeline thickness between before and after stretching, making the impact of the change in misalignment on the stress concentration coefficient k_j relatively gentle.

In the finite element analysis process, the maximum stress of the specimen was located at the weld root, which was consistent with the actual results of the welding tests (shown in Figure 5).

Figure 5. Fatigue crack.

3.2. Stress Concentration Factor under Different Welding Conditions

By comparing the structural stress concentration factor k_j, obtained from the finite element simulation of GMAW (5G, i.e., all position for pipe) without backing, with the total stress concentration factor k, as shown in Figure 6, it can be seen that the distributions of k_j and k were roughly similar, and that most values of k were below those of k_j under the same misalignment condition. It is noticed that when the misalignment was small (less than 0.5 mm), k was larger than k_j. This was because, when the material properties were set, the material properties of the heat affected zone were set to be the same as those of the base material. However, in reality, the microstructure of the heat affected zone undergoes drastic changes, and its material properties may differ slightly from those of the base material. Thus, when the misalignment was small, the structural changes in the heat affected zone significantly affected the stress concentration coefficient, making k larger than k_j. However, when the misalignment was large (more than 0.5 mm), it played a dominant role in the stress concentration coefficient, and the influence of structural changes in the heat affected zone was reduced, so the distribution rules of k and k_j tended to be consistent. In the actual welding process, due to the limited fitting-up accuracy of large pipelines, the misalignment is usually more than 0.5 mm, so the impact of this error is minimal. Therefore, this non-destructive method of analysis using the finite element method can be used to calculate the stress concentration factor, and the subsequent fatigue performance prediction can be analyzed through k_j with a larger safety coefficient.

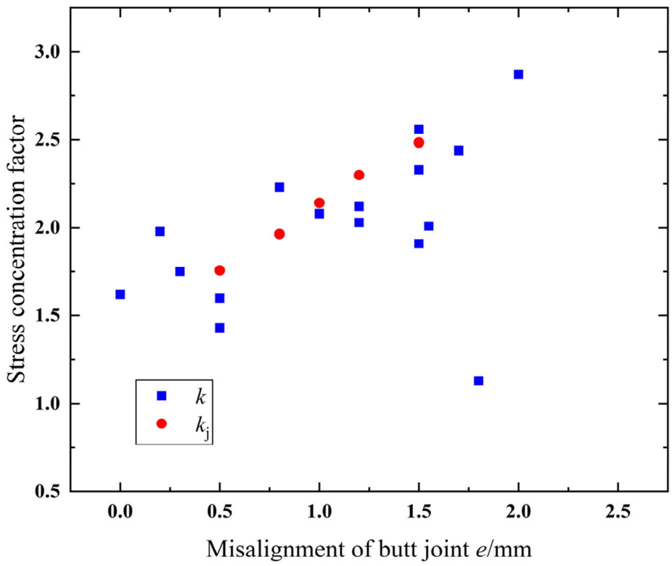

Figure 6. Comparison of k_j and k for GMAW (5G) without backing.

To analyze the effects of different misalignments on k_m and k_t, experiments were conducted on five welding processes at 5G position (as listed in Table 6). For each welding process, calculations were performed on butt joints with three misalignment conditions of 0 mm, 1.0 mm, and 2.0 mm, respectively. The calculation results are shown in Figure 7.

Table 6. Welding parameters at typical positions for different welding processes.

Welding Processes	Position	Current (A)	Voltage (V)	Welding Speed (mm/s)
RMD 5G	12 o'clock	251	16.2	7.2
	3 o'clock	261	17.7	8.2
	6 o'clock	271	17.7	8.2
GMAW 5G backing	12 o'clock	170	30.3	8.4
	3 o'clock	180	33.3	9.2
	6 o'clock	190	33.3	9.2

Table 6. *Cont.*

Welding Processes	Position	Current (A)	Voltage (V)	Welding Speed (mm/s)
GMAW 5G without backing	12 o'clock	170	30.3	8.4
	3 o'clock	180	33.3	9.2
	6 o'clock	190	33.3	9.2
AUTO TIG 5G	12 o'clock	82	10.2	1.2
	3 o'clock	88	11.2	1.5
	6 o'clock	94	12.2	1.5
TIP TIG 5G	12 o'clock	130	13.5	3.8
	3 o'clock	138	14.5	4.3
	6 o'clock	146	15.5	4.3

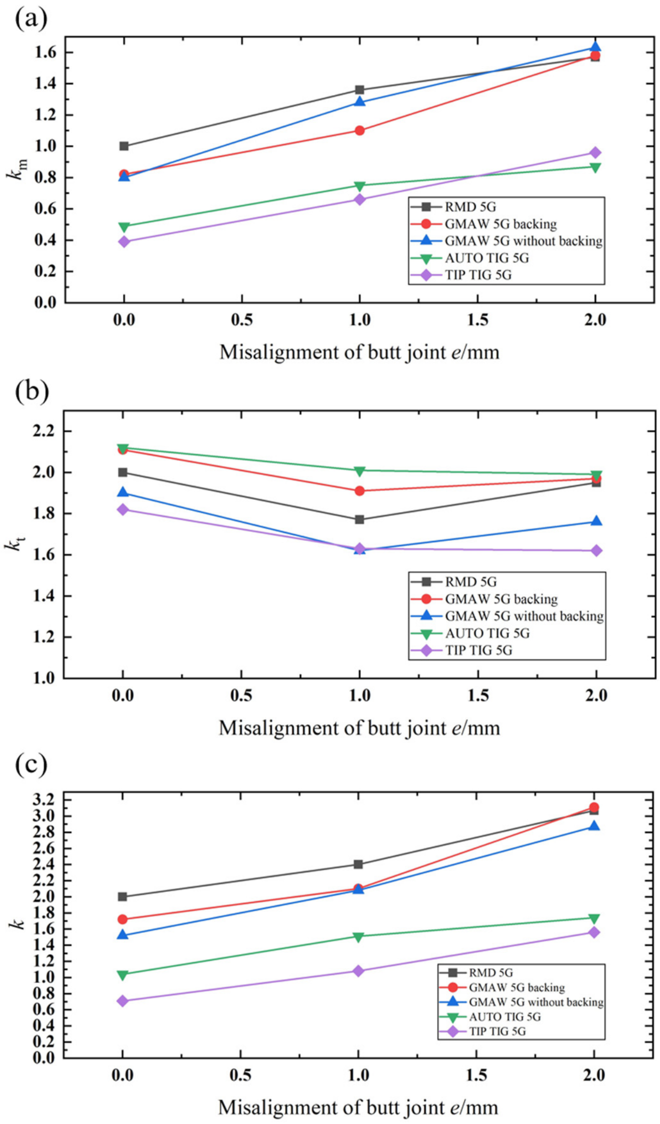

Figure 7. Stress concentration factors for various welding processes. (**a**) k_m; (**b**) k_t; (**c**) k.

From the calculation results in Figure 7, the stress concentration factor k_m gradually increased with an increase in misalignment, while the equivalent notch stress concentration factor k_t, caused by weld shape, did not change significantly with the increase in misalignment, and the k_t of each welding processes fluctuated steadily within a small range. The notch stress concentration factor k_t is used to describe the stress distribution near the notch when there is a notch in the stress field, mainly influenced by factors such as notch size, shape, and material properties. More welding tests were performed on GMAW

(5G) without backing, and the fluctuation range of k_t was 1.6–2.0 (as shown in Figure 8). The equivalent notches generated by misalignments in these tests did not change with the increase in misalignment. This is because the misalignment was small, while the pipe wall thickness was large. During welding, the molten metal was able to smoothly connect the misalignment under the action of surface tension, forming a smooth equivalent notch. Thus, the impact of misalignment on the equivalent notch was not significant. At the same time, the misalignments of RMD (regulated metal deposition) (5G), GMAW (5G) with backing, and GMAW (5G) without backing had a significant impact on k_m (Figure 7a); the misalignments of AUTO TIG (tungsten inert gas) (5G) and AUTO TIP TIG (technologie ingenieur plasch TIG) (5G) had a relatively small impact on k_m (Figure 7a). This is because the heat inputs of TIG and TIP TIG were relatively small, and the welding deformation and residual stress caused by misalignment were also relatively small. High heat input leads to a rapid heating and cooling of the weld joint and its surrounding area, resulting in increased deformation of the weld joint and its surrounding area, thereby increasing the stress concentration factor. This indicates that the stress concentration factor can be significantly reduced if TIG or TIP TIG welding processes are employed, suggesting an improved fatigue performance.

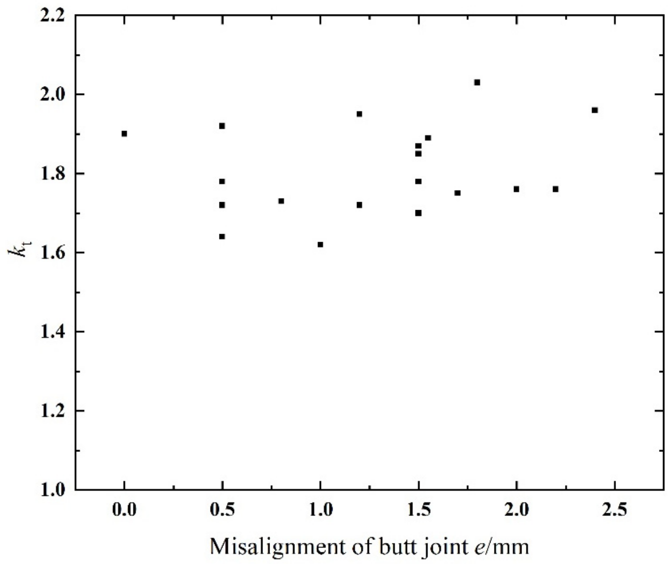

Figure 8. Misalignment and equivalent notch stress concentration factor k_t in GMAW (5G).

3.3. Fatigue Performance Prediction of Weld Joints with Misalignment

To verify the correspondence between the stress concentration factor k_j and the fatigue performance of the weld joints, fatigue tests were conducted on samples of GMAW (5G) without backing. The fatigue load was loaded axially, with a static load of 400.0 MPa and a dynamic load of 175.0 MPa. The main standards used in the experiment were DEP-37.81.40.31-Gen: 2013 [28], BS EN ISO 5817: 2014 [32], BS EN ISO 6520-1: 2007 [33], etc. The experimental results are shown in Table 7.

Table 7. Fatigue life of different misalignments.

Misalignment e/mm	Fatigue Life N/cycles
0	784,839
1.0	559,642
2.0	262,502

Zhou et al. [34] used machine learning methods to predict fatigue life. By using various mechanical data, such as axial stress, axial strain, and shear stress, from different parts as input data, and fatigue life as output data, the prediction effect was ideal. Therefore, it can be considered that there is a relationship between the stress concentration factor and fatigue life.

The structural stress concentration factor k_j and fatigue life can be fitted into a linear function by using the least squares method, as shown in Figure 9.

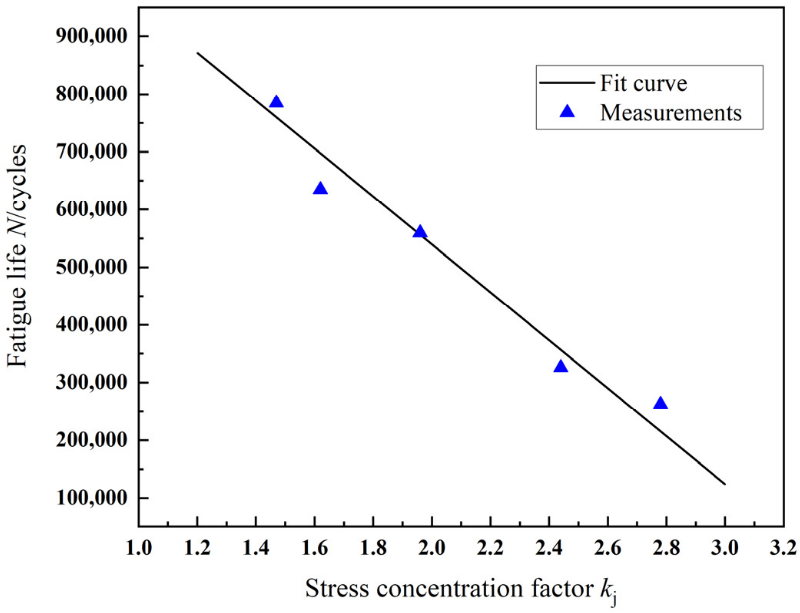

Figure 9. Fitting results of the structural stress concentration factor k_j and fatigue life.

The curve parameters for Figure 9 and relative errors are shown in Table 8. The structural stress concentration factor k_j of the weld joint had a good correlation with the fatigue life, and the relative error of the fitting result was relatively small at less than 10%. Therefore, the prediction of the fatigue life of weld joints with misalignments can be achieved by using finite element modeling combined with the structural stress calculation.

Table 8. Fitting curve parameters of the structural stress concentration factor k_j and fatigue life.

Coefficient for Linear Term	Coefficient for Constant Term	Relative Error
−415,630.53	1,370,972.88	<10%

4. Conclusions

This work uses the structural stress method to model and calculate the structural stress concentration factor k_j of weld joints with misalignments, verifies the accuracy of the calculation results with the total stress concentration factor k, and uses it to predict the fatigue performance of weld joints with misalignments. The main conclusions are as follows:

- The finite element method can be used to model weld joints with different misalignments, and to calculate the structural stress concentration factor. The misalignment e of the weld joint and the structural stress concentration factor k_j can be fitted into a quadratic function, with a residual sum of squares of 2.384×10^{-17}.
- By calculating the stress concentration factor of the weld joint, it can be found that the distribution of k_j is roughly similar to that of the total stress concentration factor k, and most values of k are smaller than those of k_j. The main parameter affecting the stress concentration factor of the weld joint is the stress concentration factor caused by misalignment k_m.
- Fatigue tests on weld joints showed that there is a linear relationship between the structural stress concentration factor k_j and fatigue life. Finite element analysis com-

bined with the structural stress method can predict the fatigue performance of weld joints with misalignments.
- Choosing TIG or TIP TIG welding processes with a smaller k_m can significantly reduce the stress concentration factor and help improve the fatigue life of weld joints.

Author Contributions: Conceptualization, C.D.; methodology, N.Z. and Z.L.; software, Z.L.; validation, Z.L. and S.W.; formal analysis, N.Z., C.D. and Z.W.; investigation, N.Z.; resources, C.D.; data curation, N.Z. and Z.L.; writing—original draft preparation, N.Z.; writing—review and editing, C.D., Z.L., Z.W. and S.W.; supervision, C.D. All authors have read and agreed to the published version of the manuscript.

Funding: This research received no external funding.

Data Availability Statement: The raw data supporting the conclusions of this article will be made available by the authors on request.

Acknowledgments: We would like to acknowledge Dongpo Wang for his contributions to the conceptualization, methodology, and resources.

Conflicts of Interest: Author Niantao Zhang is employed by the company Offshore Oil Engineering Co., Ltd. The remaining authors declare that the research was conducted in the absence of any commercial or financial relationships that could be construed as a potential conflict of interest.

References

1. Cheng, C.M. Butt-welding residual stress of heat treatable aluminum alloys. *J. Mater. Sci. Technol.* **2007**, *23*, 217–222.
2. Teng, T.L.; Fung, C.P.; Chang, P.H. Analysis of residual stresses and distortions in T-joint fillet welds. *Int. J. Pres. Ves. Pip.* **2001**, *78*, 523–538. [CrossRef]
3. Ma, W.; Bai, T.; Li, Y.; Zhang, H.; Zhu, W. Research on improving the accuracy of welding residual stress of deep-sea pipeline steel by blind hole method. *J. Mar. Sci. Eng.* **2022**, *10*, 791. [CrossRef]
4. Halabuk, D.; Návrat, T. Determination of residual stresses in cylindrical components by the hole-drilling method. *Exp. Mech.* **2022**, *62*, 87–99. [CrossRef]
5. *ASTM E837*; Standard Test Method for Determining Residual Stresses by the Hole-Drilling Strain-Gage Method. American Society for Testing and Materials: West Conshohocken, PA, USA, 2020.
6. Hong, L.; Zhe, J.; Dan, P. Study about the technique of determining residual stress of loading measuring method. *Adv. Mech. Eng.* **2021**, *13*, 168781. [CrossRef]
7. Tajdary, P.; Morin, L.; Braham, C. A deconvolution method for the mapping of residual stresses by X-ray diffraction. *Exp. Mech.* **2022**, *62*, 1349–1362. [CrossRef]
8. Li, Y.; Wu, J.; Qiang, B. Measurements of residual stresses in a welded orthotropic steel deck by the hole-drilling method considering stress biaxiality. *Eng. Struct.* **2021**, *23*, 111690. [CrossRef]
9. Nitschke-Pagel, T. Recommendations for the measurement of residual stresses in welded joints by means of X-ray diffraction results of the WG6-RR test. *Weld. World.* **2021**, *65*, 589–600. [CrossRef]
10. Eftekhar, S. Welding simulation of X70 oil and gas pipeline sheet using various heat sources and experimental validation. *IOSR J. Eng.* **2017**, *7*, 23–31.
11. Maarten, R.; Richard, P.; Henk, S. A combined experimental and numerical examination of welding residual stresses. *J. Mater. Sci. Technol.* **2018**, *261*, 98–106.
12. Venkata, K.A.; Kumar, S.; Dey, H.C. Study on the effect of post weld heat treatment parameters on the relaxation of welding residual stresses in electron beam welded P91 steel plates. *Proc. Eng.* **2014**, *86*, 223–233. [CrossRef]
13. Xu, S.; Chen, J.; Shen, W. Fatigue strength evaluation of 5059 aluminum alloy welded joints considering welding deformation and residual stress. *Int. J. Fatigue* **2022**, *162*, 106988. [CrossRef]
14. Cheng, Y.; Wang, H. Finite element analysis of welding residual stress in long distance gas pipeline. *Earth Env. Sci.* **2021**, *687*, 012105.
15. Zhao, W.; Jiang, W.; Zhang, H. 3D finite element analysis and optimization of welding residual stress in the girth joints of X80 steel pipeline. *J. Manuf. Process.* **2021**, *66*, 166–178. [CrossRef]
16. *NF EN 1993-1-9*; Eurocode 3: Design of Steel Structures-Part 1–9: Fatigue. European Committee for Standardization: Brussels, Belgium, 2005.
17. Hänel, B.; Haibach, E.; Seeger, T.; Wirthgen, G.; Zenner, H. *FKM-Guideline-Analytical Strength Assessment of Components in Mechanical Engineering (Technical Report)*; Forschungskuratorium Maschinenbau (FKM): Frankfurt, Germany, 2003.
18. Koçak, M.; Hadley, I.; Szavai, S.; Tkach, Y.; Taylor, N. *FITNET Fitness-for-Service (FFS) Procedure-Volume 1, Revision mk8 (Technical Report)*; GKSS Research Centre: Geesthacht, Germany, 2008.
19. *NF EN 13445-3 V1*; Unfired Pressure Vessels-Part 3: Design. European Committee for Standardization: Brussels, Belgium, 2014.

20. Rao, S.S.D.; Raju, S. Orthogonalized generalized ISO-geometric analysis (OGIGA) and its applications to problems of fracture mechanics. *Comput. Methods Appl. Mech. Eng.* **2020**, *372*, 113427. [CrossRef]
21. Jiang, W.C.; Xie, X.F.; Wang, T.J.; Zhang, X.C.; Zhao, X. Fatigue life prediction of 316L stainless steel weld joint including the role of residual stress and its evolution: Experimental and modelling. *Int. J. Fatigue* **2021**, *143*, 105997. [CrossRef]
22. Pokorny, P.; Dlhy, P.; Poduska, J.; Fajkos, R.; Vojtec, T.; Nahlik, L.; Grasso, M.; Hutar, P. Influence of heat treatment-induced residual stress on residual fatigue life of railway axles. *Theor. Appl. Fract. Mec.* **2020**, *109*, 102732. [CrossRef]
23. Barsoum, Z.; Barsoum, I. Residual stress effects on fatigue life of welded structures using LEFM. *Eng. Fail. Anal.* **2009**, *16*, 449–467. [CrossRef]
24. Cui, C.; Zhang, Q.; Bao, Y. Fatigue life evaluation of welded joints in steel bridge considering residual stress. *J. Constr. Steel Res.* **2019**, *153*, 509–518. [CrossRef]
25. Fricke, W. IIW guideline for the assessment of weld root fatigue. *Weld. World* **2013**, *57*, 753–791. [CrossRef]
26. Niemi, E.; Fricke, W.; Maddox, S.J. *Fatigue Analysis of Welded Components-Designer's Guide to the Structural Hot-Spot Stress Approach (IIW-1430-00)*; Woodhead Publishing: Cambridge, UK, 2006.
27. Mitra, A.; Siva Prasad, N.; Janaki Ram, G.D. Influence of temperature and time of post-weld heat treatment on stress relief in an 800-mm-thick steel weldment. *J. Mater. Eng. Perform.* **2016**, *25*, 1384–1393. [CrossRef]
28. *DEP 37.81.40.31-Gen*; Welding of Deepwater Pipelines, Flowlines and Steel Catenary Risers (Amendments and Supplements to API 1104). Shell: London, UK, 2013.
29. Dong, P. A structural stress definition and numerical implementation for fatigue analysis of welded joints. *Int. J. Fatigue* **2001**, *23*, 865–876. [CrossRef]
30. Hobbacher, A. *Recommendations for Fatigue Design of Welded Joints and Components*; Springer International Publishing: Berlin/Heidelberg, Germany, 2007.
31. Pachoud, A.J.; Manso, P.A.; Schleiss, A.J. New parametric equations to estimate notch stress concentration factors at butt welded joints modeling the weld profile with splines. *Eng. Fail. Anal.* **2017**, *72*, 11–24. [CrossRef]
32. *ISO 5817*; Welding—Fusion-Welded Joints in Steel, Nickel, Titanium and Their Alloys (Beam Welding Excluded)—Quality Levels for Imperfections. International Organization for Standardization: Geneva, Switzerland, 2014.
33. *ISO 6520-1*; Welding and Allied Processes—Classification of Geometric Imperfections in Metallic Materials—Part 1: Fusion Welding. International Organization for Standardization: Geneva, Switzerland, 2007.
34. Zhou, K.; Sun, X.; Shi, S. Machine learning-based genetic feature identification and fatigue life prediction. *Fatigue Fract. Eng. Mater. Struct.* **2021**, *44*, 2524–2537. [CrossRef]